Disentangling the surface and bulk electronic structures of LaOFeAs

P. Zhang,[1] J. Ma,[1] T. Qian,[1,2] Y. G. Shi,[1] A. V. Fedorov,[3] J. D. Denlinger,[3] X. X. Wu,[1]
J. P. Hu,[1,2,4] P. Richard,[1,2,*] and H. Ding[1,2,†]

[1]*Beijing National Laboratory for Condensed Matter Physics, and Institute of Physics, Chinese Academy of Sciences, Beijing 100190, China*
[2]*Collaborative Innovation Center of Quantum Matter, Beijing, China*
[3]*Advanced Light Source, Lawrence Berkeley National Laboratory, Berkeley, California 94720, USA*
[4]*Department of Physics, Purdue University, West Lafayette, Indiana 47907, USA*

We performed a comprehensive angle-resolved photoemission spectroscopy study of the electronic band structure of LaOFeAs single crystals. We found that samples cleaved at low temperature show an unstable and highly complicated band structure, whereas samples cleaved at high temperature exhibit a stable and clearer electronic structure. Using *in situ* surface doping with K and supported by first-principles calculations, we identify both surface and bulk bands. Our assignments are confirmed by the difference in the temperature dependence of the bulk and surface states.

I. INTRODUCTION

Despite an earlier study [1] reporting superconductivity at 5 K in LaOFeP with the so-called 1111 crystal structure, the discovery of a superconducting critical temperature T_c of 26 K in F-doped LaOFeAs [2,3] with the same structure is generally used to mark the beginning of the era of the Fe-based superconductors. Up to now the 1111 family is still the one exhibiting the highest T_c's in bulk single crystals at ambient pressure among all Fe-based superconductors [4,5]. Understanding why high-T_c superconductivity is favored in this system is important but requires a good characterization of its electronic structure. However, the 1111 samples show a polarized cleaved surface that results from both $[LaO]^{+1}$ and $[FeAs]^{-1}$ surface termination layers. This leads to a surface reconstruction after cleaving [6,7]. One possible reconstruction involves $0.5e$ charge transfer from the bottom surface layer to the top surface layer [6], as illustrated in Fig. 1(a), which resembles the polar surface issue encountered in the $YBa_2Cu_3O_{7-\delta}$ system [8]. Consequently, the coexistence of surface and bulk electronic states complicates the measurement of the intrinsic electronic structure by angle-resolved photoemission spectroscopy (ARPES) [9–15]. Previous reports show very complicated band structures, and lack of direct and definite evidences to separate the surface and bulk bands.

In this paper, we present a detailed investigation by ARPES of the electronic band structure of the parent compound LaOFeAs. We show that the band structure depends on the sample cleaving temperature, possibly due to surface reconstruction. In particular, high-temperature cleaving produces a clean and stable band structure. Supported by local density approximation (LDA) calculations, we distinguish both surface and bulk states. Upon doping the surface *in situ* with K, we clearly observe different energy shifts of surface and bulk states on both the core levels and the valence states. We also use temperature-dependent measurements to show that the surface and bulk states evolve differently,

thus confirming their assignment. Our results provide a good starting point for extracting the key ingredients responsible for the high T_c of the 1111 ferropnictide superconductors.

II. EXPERIMENT

High-quality single crystals of LaOFeAs were grown with NaAs flux. This material shows a structural transition at $T_S =$ 155 K and a magnetic transition at about $T_S =$ 137 K [2,16]. ARPES measurements were performed at the Advanced Light Source, beamlines BL12 and BL4, using VG-Scienta electron analyzers. The energy resolution was set to 15 meV and the angular resolution was set to $0.2°$. The experimental geometry is shown in Fig. 1(b). All measurements of the valence bands presented in this paper were performed at 80 eV, except mentioned otherwise. Clean surfaces for the ARPES measurements were obtained by cleaving the samples *in situ* in a working vacuum better than 7×10^{-11} Torr. We use the tight binding model in Ref. [17] with a manual shift of onsite energies and hopping parameters for the d_{xy} and d_{z^2} orbitals to match the experimental data.

III. IMPACT OF THE CLEAVING TEMPERATURE

We found that the observed band structure of LaOFeAs is strongly affected by the sample cleaving temperature. In Fig. 2, we compare the band structure measured on samples cleaved at 15 and 170 K, and show their evolution with recording time. We notice extra bands for the samples cleaved at 15 K as compared to the samples cleaved at 170 K, as well as band shifts with the recording time. The different band structures and their evolution with recording time are sketched in Figs. 2(c) and 2(f). The band structure of the samples cleaved at 15 K evolves with time towards the one obtained on the samples cleaved at 170 K, indicating that there is a slow reconstruction on the cleaved surfaces that relaxes much faster at high temperature.

The bands marked with dashed lines in Fig. 2(c) in the low-temperature cleaved samples disappear in the high-temperature cleaved samples, while the very large outer hole band centered at Γ is nearly unaffected, suggesting that
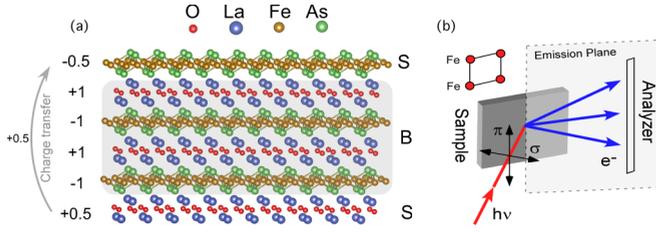
---
*p.richard@iphy.ac.cn
†dingh@iphy.ac.cn

FIG. 1. (a) Schematic drawing showing the possible charge transfer on the polarized surface. S and B on the right side stand for surface and bulk components, respectively. (b) ARPES experimental geometry. All the data in this paper are recorded along the Γ-M (Fe-Fe) direction. The geometries with linear horizontal and linear vertical polarized light are labeled σ and π, respectively.

over-hole doping at the surface persists in the high-temperature cleaved samples. This indicates the existence of more than one set of surface states. We sort the surface states in the low-temperature cleaved samples into two sets: (i) the bands of Set 1 shift with time and are absent in the high-temperature cleaved samples. They likely come from a surface reconstruction; (ii) Set 2 is stable in both low-temperature and high-temperature cleaved samples, and originates from the polarized surface.
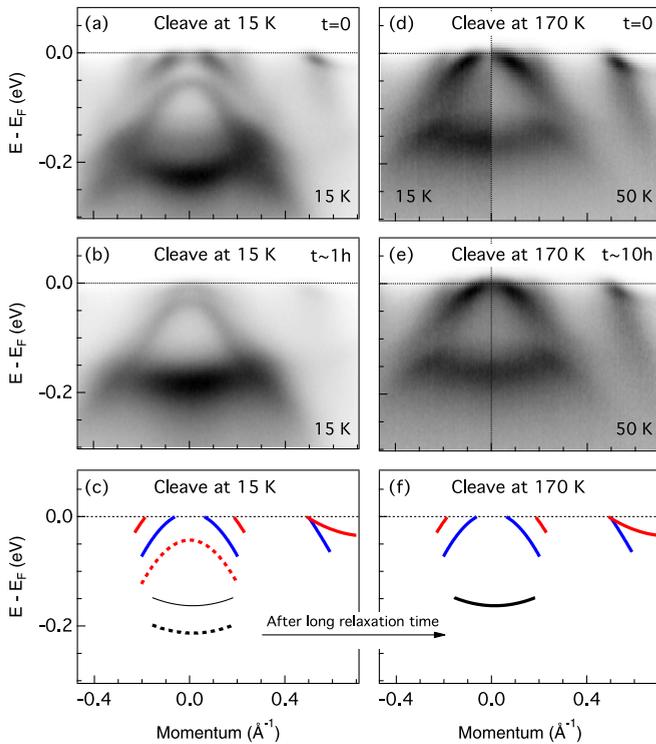

FIG. 2. (a) ARPES intensity plot of the band structure of one sample cleaved at 15 K. The data are recorded at 15 K, at the Γ point and with σ polarization. (b) Same as (a), but recorded 1 h later. (c) Cartoon of the band structure of samples cleaved at 15 K. The dashed lines indicate bands very sensitive to time. (d) Same as (a), but with one sample cleaved at 170 K. The data on the left side are recorded at 15 K and the ones on the right side are obtained at 50 K. (e) Same as (d), but recorded 10 h later, at 50 K. (f) Cartoon of the band structure of samples cleaved at 170 K.

With surface reconstructing with time, the band structure of the low-temperature cleaved samples becomes more bulklike, and the surface states associated with Set 1 finally merge with the bulk bands. In contrast, we did not observe any significant change after 10 h of measurements for the samples cleaved at 170 K, where only Set 2 is detected. However, we notice a slight band shift between data recorded at 15 and 50 K, which will be discussed below in Sec. V. We conclude that the surfaces obtained by cleaving the samples at high temperature are more representative of the intrinsic properties of LaOFeAs, where only surface states of Set 2 originating from the polarized surface exist. Therefore, we focus mainly on the samples cleaved at 170 K.

The band structure of samples cleaved at 170 K is shown in Fig. 3. From the FS mapping in Fig. 3(a), we distinguish one large FS and two small FSs at the Γ point, as well as four symmetric hot spots near M. From the band structure along high-symmetry lines corresponding to cut No. 1, cut No. 2, and cut No. 3 in Figs. 3(b)–3(d), we distinguish nine bands, which are sketched in Fig. 3(d). The very large hole FS actually consists of two bands, labeled b5 and b6. These two degenerate hole FSs are too large to account for the bulk doping and should thus be related to surface states induced by the charge transfer on the polar surface, as discussed below. The bands b1, b2, and b3 at Γ are consistent with the bulk calculations of the three t_{2g} orbitals, as shown in Fig. 3(e).

Since there is no report on orbital order in 1111 materials until now, we choose a model without orbital order to explain the band structure at the M point. After comparison with the LDA calculations, we assign bands b7 and b8 to the d_{yz} and d_{xz} bands, while band b9 corresponds to the d_{xy} hole band. The electron band with the d_{xy} orbital is not observed, similarly to many cases in Fe-based superconductors [22].

We mark the observed bands in the LDA calculations in Fig. 3(e). The bands not observed experimentally are drawn with dashed lines. If we count the FS volume of the two degenerate hole FSs (b5/b6), we find $2 \times 0.35e$/Fe using the Luttinger theorem, which is much larger than the maximum charge transfer 0.5e/Fe induced by the polar surface, as shown in Fig. 1(a). We speculate that the two hole FSs may come from different layers, or that there are some unobserved surface electron bands [13].

IV. *in situ* K DOPING

Evaporating K *in situ* on the surface of samples is a technique that has been proved useful to electron-dope surfaces of high-temperature superconductors [8,23]. It has also been used to kill some surface states in the Fe-based superconductors [24]. Na deposition was previously used to separate surface and bulk bands [13]. However, most bands were killed by a large Na dose (10 s for one monolayer) in that study. With a high-precision K dispenser, here we deposit only a small amount of K in sequences (less than one monolayer in total) to study the shifts of different bands, and thus to distinguish the surface and bulk components of the measured electronic structure. We first investigate the core level shifts with K doping time. Since the chemical environments at the surface and in the bulk are different due to the polar surface of LaOFeAs, the surface and bulk core levels should be different.
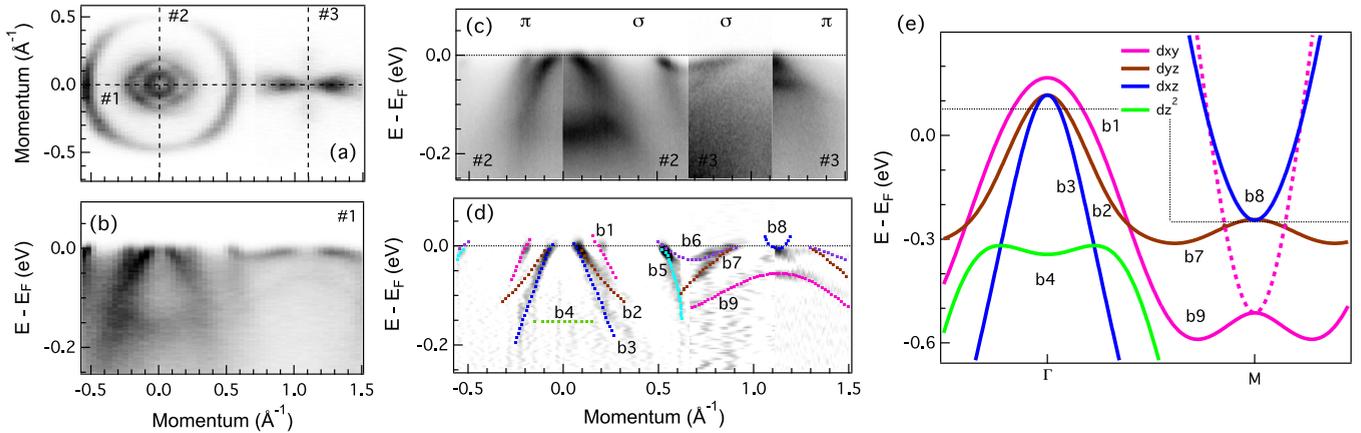
FIG. 3. (a) FS mapping at 15 K with data from $\sigma + \pi$ polarization. (b) ARPES intensity plot of the band structure along cut No. 1 from panel (a). The intensity between $k_x = (0.71, 1.5)$ in (a) is multiplied by 2 to show the details near M. (c) ARPES intensity plots of the band structure along cuts No. 2 and No. 3, with different polarizations. The visibility of the d_{z^2} band with the σ polarization is caused by a sizable component A_z of the potential vector perpendicular to the sample surface in our experimental setup, for which p_z and d_{z^2} bands are particularly sensitive [18]. (d) Curvature intensity plot [19] of (c) and sketch of the band structure. (e) LDA calculations. The solid lines are the ones observed in the experimental data, whereas the dashed line corresponds to the band not observed. The horizontal dashed lines correspond approximately to the experimental Fermi level [20,21].

Indeed, we see in Fig. 4(a) that the As $3d_{3/2}$ and As $3d_{5/2}$ core levels split into four peaks, labeled from P1 to P4. For a quantitative understanding, we fit the peaks with Lorentzian functions. The extracted peak positions and areas are shown in Fig. 4(b). We find that P1 and P3 on one hand, and P2 and P4 on the other hand, form two pairs with a fixed peak intensity ratio, suggesting that one set of peaks belongs to the surface states whereas the other pair is associated with the bulk. While the positions of the P1 and P3 peaks do not change with K doping time, the positions of the P2 and P4 peaks move to higher binding energy, in agreement with an electron doping. Since surface states are more sensitive to *in situ* K doping, we

assign the P2 and P4 peaks to surface states, and attribute the P1 and P3 peaks to bulk states.

Next we use K doping to study the evolution of the valence states. The band structures before and after K doping are shown in Figs. 4(c) and 4(d) and Figs. 4(e) and 4(f), respectively. With the help of lines No. L2 and No. L3 [see Figs. 4(c) and 4(d) for the momentum locations], we found that except for the broadening caused by the disordered K atoms, the most obvious change is the large downward shift of the bands b5/b6, while other bands have no obvious shifts. More precisely, we extracted the band dispersions of easily traceable bands before K doping and superimposed them on plots after K doping
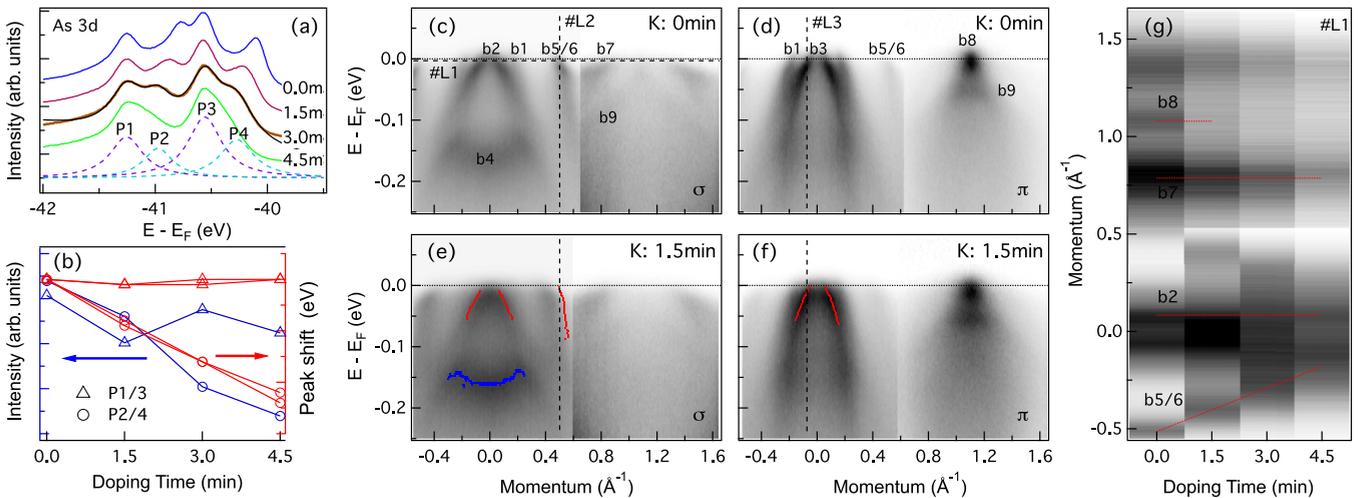

FIG. 4. (a) Core levels of As $3d$ as a function of K doping time. The black line is a fitting of the core levels after 3-min K doping. The fitting uses a sum of four Lorentzian functions. The dashed purple and light blue lines are the fittings of individual peaks. Due to the spin-orbit coupling, the As $3d$ core levels split into $3d_{3/2}$ and $3d_{5/2}$ peaks, with a 2:3 intensity ratio. Thus, we fixed the area ratios P1/P3 and P2/P4 to 2:3. (b) Peak area (blue, left axis) and peak shifts (red, right axis) of P1/P3 and P2/P4, with K doping time. (c) and (d) Band structure recorded before K evaporation at 50 K with σ and π polarizations, respectively. (e) and (f) Same as (c) and (d), but recorded after K doping. The red (blue) dashed lines are the MDC (EDC) peak positions extracted from (c) and (d). (g) k_F shifts with K doping time, at $E = E_F$ [cut No. L1 in (c)].

[Figs. 4(e) and 4(f)]. We found that bands b5 and b6 indeed shift a lot, while bands b2–b4 overlap well with the one after K doping. We also notice that band b2 shows strong intensity near the band top after K doping, for which the origin is unclear. To show the band change clearly, we display the MDC change at line No. L1 [see Fig. 4(c) for the energy location] with K doping time in Fig. 4(g). A common feature in this panel is the weakening of intensity with K doping due to the disorder introduced by the K atoms. Nevertheless, our results show clearly that while the k_F position of the bands b5 and b6 shifts significantly with surface doping, the k_F positions of the bands b2, b7, and b8 almost do not. As we did with the core levels, this observation indicates that the bands b5 and b6 are from the surface, while the others are more bulk representative.

V. TEMPERATURE DEPENDENCE

From the temperature evolution of the band structures displayed in Fig. 5, we notice obvious band shifts, as reported previously for other Fe-based superconductors [20,25,26]. The band shifts cannot be attributed to the aging effect since we checked the band structure at 50 K (Fig. 2) and 170 K (Fig. 5) after a thermal cycle and found no shift. Interestingly, the band shifts of the surface and bulk states with temperature are different. The outer hole bands b5 and b6 at Γ in Figs. 5(a)–5(d), which we attribute to surface states, show a large shift towards the high binding energies, whereas the bulk hole band b2 in Figs. 5(a)–5(d) and the hole band b3 in Figs. 5(e)–5(h) show a relatively small shift. We notice that the d_{z^2} band b4 almost does not shift with temperature, which differs from results shown in Ref. [13]. One explanation is that the samples in that study were cleaved at low temperature, in which case the slow surface reconstruction would exist and cause a band shift similar to the d_{z^2} band shift shown in Fig. 2.

We display the EDCs at the positions labeled No. K1, No. K2, and No. K3 at different temperatures in Figs. 5(m)–5(o). The bulk bands b2 and b3 have a shift of $50 \sim 60$ meV, while the surface band b5 has a shift of about 110 meV, about twice as large. The band shifts can be partially explained by the carrier conservation and the large decrease in the density-of-states decrease near the Fermi level (hole band top) [20]. In Figs. 5(i)–5(l) we show the band structure at different temperatures at the M point. Under π polarization, the most obvious feature is the electron band b8, which is very strong and thus has a large intensity even below E_F. The band structure under σ polarization is too weak [Figs. 4(c) and 4(e)] for the temperature dependent study and thus ignored.

VI. SUMMARY

In summary, we performed a detailed study of the band structure of the parent compound LaOFeAs. We identified two sets of surface states, one existing only in the low-temperature cleaved samples and possibly caused by a slow surface reconstruction, and another one induced by a polarized surface. We eliminated the former one by high-temperature cleaving. Although the two very large hole b5 and b6 bands remain in the high-temperature cleaved samples, we could distinguish them from bulk-representative states by doping
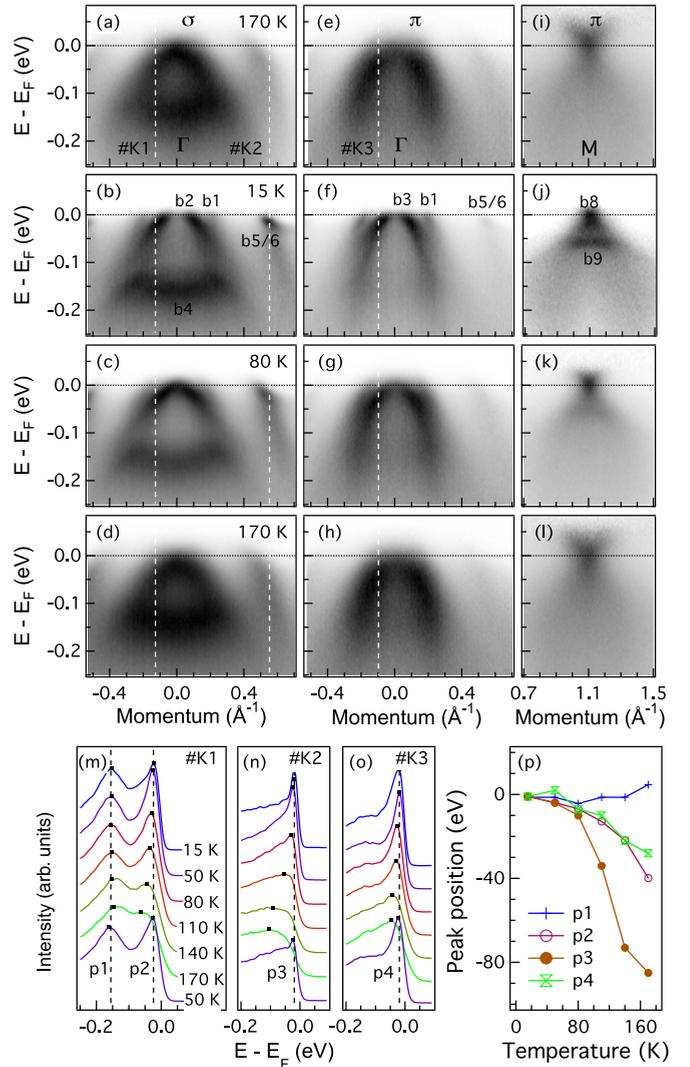

FIG. 5. (a)–(d) ARPES intensity plots recorded at Γ with σ polarization, for the temperature cycle 170 K $\rightarrow$ 15 K $\rightarrow$ 80 K $\rightarrow$ 170 K. (e)–(h) same as (a)–(d), but with π polarization. (i)–(l) Same as (e)–(h), but for a cut at M and divided by the Fermi function at the corresponding temperature. (m)–(o) Temperature evolution of the EDCs at momenta No. K1, No. K2, and No. K3, respectively. Black markers indicate the peak positions. The curves at the bottom of each panel are the EDCs at 50 K after thermal cycle. (p) Peak position shifts as a function of temperature. Labels correspond to the peaks shown in panels (m)–(o).

the surface of LaOFeAs *in situ* using K and by looking at their temperature evolution. Our results indicate a routine method for disentangling bulk and surface states in the Fe-based superconductors, and pave the way for future studies of the bulk bands in the LaOFeAs family.

[1] Y. Maeno, H. Hashimoto, K. Yoshida, S. Nishizaki, T. Fujita, J. G. Bednorz, and F. Lichtenberg, Nature (London) **372**, 532 (1994).

[2] Y. Kamihara, T. Watanabe, M. Hirano, and H. Hosono, J. Am. Chem. Soc. **130**, 3296 (2008).

[3] H. Takahashi, K. Igawa, K. Arii, Y. Kamihara, M. Hirano, and H. Hosono, Nature (London) **453**, 376 (2008).

[4] X. H. Chen, T. Wu, G. Wu, R. H. Liu, H. Chen, and D. F. Fang, Nature (London) **453**, 761 (2008).

[5] Z.-A. Ren, W. Lu, J. Yang, W. Yi, X.-L. Shen, Z.-C. Li, G.-C. Che, X.-L. Dong, L.-L. Sun, F. Zhou *et al.*, Chin. Phys. Lett. **25**, 2215 (2008).

[6] A. Pojani, F. Finocchi, J. Goniakowski, and C. Noguera, Surf. Sci. **387**, 354 (1997).

[7] J. Goniakowski and C. Noguera, Phys. Rev. B **60**, 16120 (1999).

[8] M. A. Hossain, J. D. F. Mottershead, D. Fournier, A. Bostwick, J. L. McChesney, E. Rotenberg, R. Liang, W. N. Hardy, G. A. Sawatzky, I. S. Elfimov *et al.*, Nat. Phys. **4**, 527 (2008).

[9] D. H. Lu, M. Yi, S. K. Mo, A. S. Erickson, J. Analytis, J. H. Chu, D. J. Singh, Z. Hussain, T. H. Geballe, I. R. Fisher *et al.*, Nature (London) **455**, 81 (2008).

[10] T. Kondo, A. F. Santander-Syro, O. Copie, C. Liu, M. E. Tillman, E. D. Mun, J. Schmalian, S. L. Bud'ko, M. A. Tanatar, P. C. Canfield *et al.*, Phys. Rev. Lett. **101**, 147003 (2008).

[11] D. Lu, M. Yi, S.-K. Mo, J. Analytis, J.-H. Chu, A. Erickson, D. Singh, Z. Hussain, T. Geballe, I. Fisher *et al.*, Physica C **469**, 452 (2009).

[12] H. Eschrig, A. Lankau, and K. Koepernik, Phys. Rev. B **81**, 155447 (2010).

[13] L. X. Yang, B. P. Xie, Y. Zhang, C. He, Q. Q. Ge, X. F. Wang, X. H. Chen, M. Arita, J. Jiang, K. Shimada *et al.*, Phys. Rev. B **82**, 104519 (2010).

[14] C. Liu, Y. Lee, A. D. Palczewski, J.-Q. Yan, T. Kondo, B. N. Harmon, R. W. McCallum, T. A. Lograsso, and A. Kaminski, Phys. Rev. B **82**, 075135 (2010).

[15] A. Charnukha, S. Thirupathaiah, V. B. Zabolotnyy, B. Buechner, N. D. Zhigadlo, B. Batlogg, A. N. Yaresko, and S. V. Borisenko, Sci. Rep. **5**, 10392 (2015).

[16] C. de la Cruz, Q. Huang, J. W. Lynn, J. Li, W. Ratcliff, II, J. L. Zarestky, H. A. Mook, G. F. Chen, J. L. Luo, N. L. Wang *et al.*, Nature (London) **453**, 899 (2008).

[17] S. Graser, T. A. Maier, P. J. Hirschfeld, and D. J. Scalapino, New J. Phys. **11**, 025016 (2009).

[18] P. Richard, T. Qian, and H. Ding, J. Phys.: Condens. Matter **27**, 293203 (2015).

[19] P. Zhang, P. Richard, T. Qian, Y.-M. Xu, X. Dai, and H. Ding, Rev. Sci. Instrum. **82**, 043712 (2011).

[20] V. Brouet, P.-H. Lin, Y. Texier, J. Bobroff, A. Taleb-Ibrahimi, P. Le Fevre, F. Bertran, M. Casula, P. Werner, S. Biermann *et al.*, Phys. Rev. Lett. **110**, 167002 (2013).

[21] S. V. Borisenko, D. V. Evtushinsky, Z.-H. Liu, I. Morozov, R. Kappenberger, S. Wurmehl, B. Büchner, A. N. Yaresko, T. K. Kim, M. Hoesch *et al.*, Nat. Phys. **12**, 311 (2016).

[22] P. Zhang, T. Qian, P. Richard, X. P. Wang, H. Miao, B. Q. Lv, B. B. Fu, T. Wolf, C. Meingast, X. X. Wu *et al.*, Phys. Rev. B **91**, 214503 (2015).

[23] P. Zhang, P. Richard, N. Xu, Y.-M. Xu, J. Ma, T. Qian, A. V. Fedorov, J. D. Denlinger, G. D. Gu, and H. Ding, Appl. Phys. Lett. **105**, 172601 (2014).

[24] P. Richard, C. Capan, J. Ma, P. Zhang, N. Xu, T. Tian, J. D. Denlinger, G.-F. Chen, A. S. Sefat, Z. Fisk *et al.*, J. Phys.: Condens. Matter **26**, 035702 (2014).

[25] R. S. Dhaka, S. E. Hahn, E. Razzoli, R. Jiang, M. Shi, B. N. Harmon, A. Thaler, S. L. Bud'ko, P. C. Canfield, and A. Kaminski, Phys. Rev. Lett. **110**, 067002 (2013).

[26] P.-H. Lin, Y. Texier, A. Taleb-Ibrahimi, P. Le Fèvre, F. Bertran, E. Giannini, M. Grioni, and V. Brouet, Phys. Rev. Lett. **111**, 217002 (2013).